Plasma 2
Lecture 6: Quasilinear Theory (Part II)

APPH E6102y
Columbia University

Quasilinear Vlasov-Poisson

Quasi-linear part…

$$\frac{\partial}{\partial v_z}\left\langle f_{s1}\frac{\partial \Phi_1}{\partial_z}\right\rangle = -\frac{\pi}{L}\frac{\partial}{\partial v_z}\int_{-\infty}^{\infty} \mathrm{i}k\tilde{\Phi}_1(-k,t)\tilde{f}_{s1}(k,v_z,t)\,\mathrm{d}k. \qquad (11.1.35)$$

Quasilinear Vlasov-Poisson

$$\tilde{\Phi}(x,t) = \int \frac{d\omega}{2\pi} \sum_k \Phi_k e^{-j\omega t} e^{+jkx}$$

$\omega(k)$ ~ DISPERSION RELATION

$\tilde{\Phi}^*(x,t) = \tilde{\Phi}(x,t)$ ~ A REAL NUMBER

$$= \int \frac{d\omega}{2\pi} \sum_k \Phi_k^* e^{+j\omega^* t} e^{-jkx} \qquad k \to -k$$

or $\Phi_k^* = \Phi_{-k}$

$\omega^*(k) = -\omega(-k)$

$\omega_R^*(k) = -\omega_R(-k)$

$\omega_I^*(k) = +\omega_I(-k)$

$$f_k = \frac{e}{m} \frac{k \Phi_k}{\omega - kv} \frac{\partial \langle f \rangle}{\partial v}$$

$$\Phi_{-k} f_k = \frac{ek}{m} \frac{|\Phi_k|^2}{\omega - kv} \frac{\partial \langle f \rangle}{\partial v}$$

$$\sum_k \frac{|\Phi_k|^2}{\omega(k) - kv} = \sum_k \frac{|\Phi_k|^2}{\omega_R(k) - kv + i\omega_I(k)} = \sum_k \frac{|\Phi_k|^2 [(\omega_R - kv) - i\omega_I(k)]}{(\omega_R - kv)^2 + \omega_I^2}$$

REAL PART IS ODD IN k

IMAGINARY PART IS EVEN

Quasilinear Velocity-Space Diffusion

$$\frac{\partial}{\partial t}\langle f_s\rangle(v_z,t) = \frac{\partial}{\partial v_z}\left[D_{\mathrm{q}}(v_z,t)\frac{\partial}{\partial v_z}\langle f_z\rangle(v_z,t)\right], \qquad (11.1.44)$$

$\sim (e/m)^2\, \tau_{cor}\, |E^2|$

$$D_{\mathrm{q}}(v_z,t) = \frac{2}{\epsilon_0}\left(\frac{e_s}{m_s}\right)^2 \int_{-\infty}^{\infty} \frac{\mathrm{i}\mathscr{E}(k,t)}{\omega - kv_z}\,\mathrm{d}k \qquad (11.1.45)$$

where $\mathscr{E}(k,t) = (\pi\epsilon_0/2L)|\tilde{E}_1(k,t)|^2$ is called the *spectral density* of the electric field.

$$\frac{\partial \mathscr{E}(k,t)}{\partial t} = 2\gamma(k,t)\mathscr{E}(k,t), \qquad (11.1.43)$$

Quasilinear Velocity-Space Diffusion

$$\frac{\partial}{\partial t}\langle f_s\rangle(v_z,t)=\frac{\partial}{\partial v_z}\left[D_{\rm q}(v_z,t)\frac{\partial}{\partial v_z}\langle f_z\rangle(v_z,t)\right], \tag{11.1.44}$$

$$D_{\rm q}(v_z,t)=\frac{2}{\epsilon_0}\left(\frac{e_s}{m_s}\right)^2\int_{-\infty}^{\infty}\frac{\mathscr{E}(k,t)\gamma(k,t)}{[\omega_{\rm r}(k,t)-kv_z]^2+\gamma^2(k,t)}\,{\rm d}k, \tag{11.1.47}$$

$$\frac{\partial\mathscr{E}(k,t)}{\partial t}=2\gamma(k,t)\mathscr{E}(k,t), \tag{11.1.43}$$

Many Wave-Particle Resonances

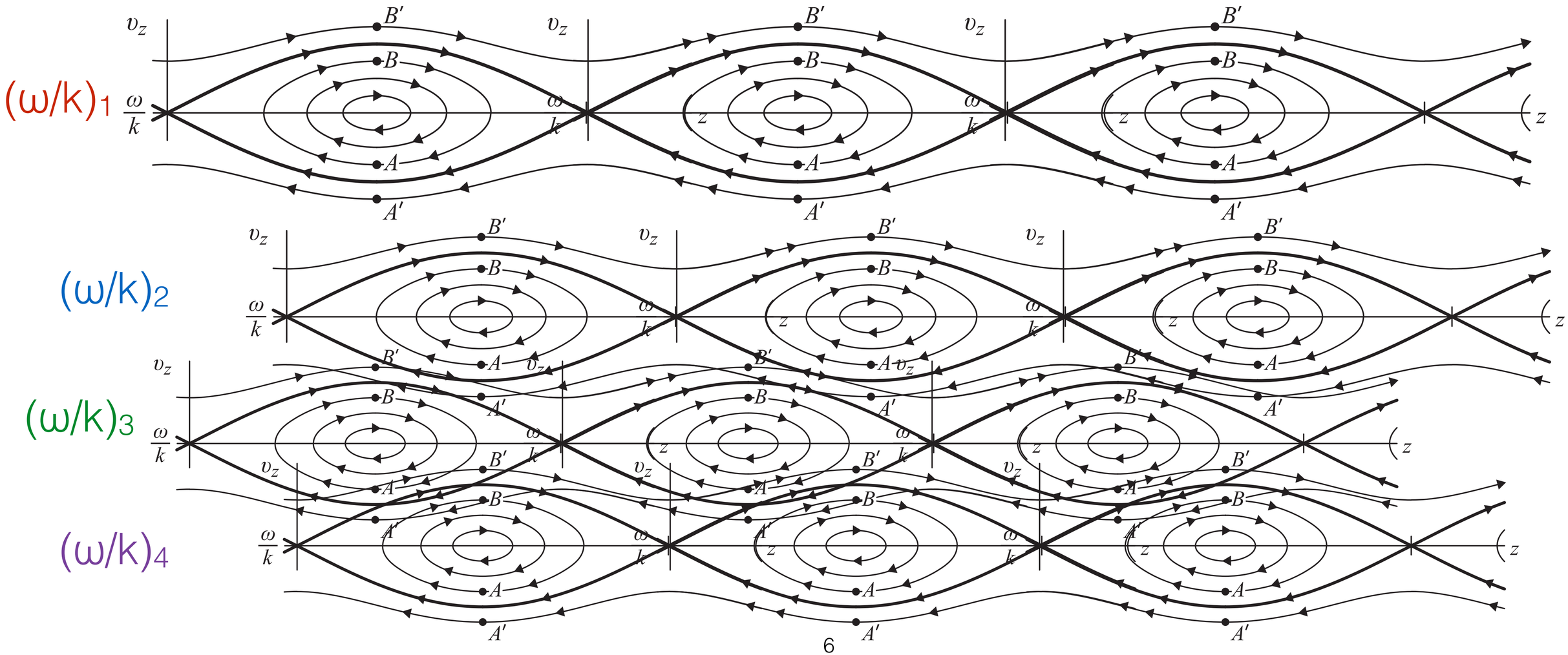

Quasilinear Velocity-Space Diffusion

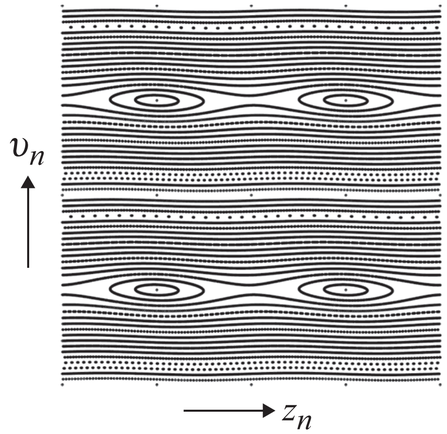

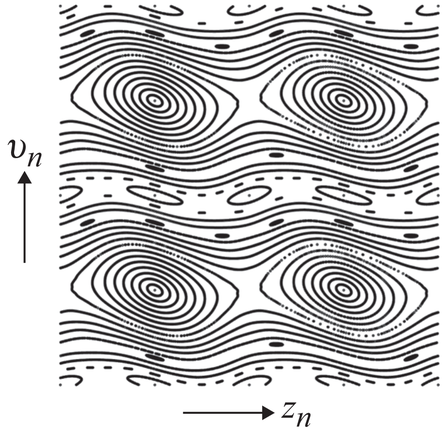

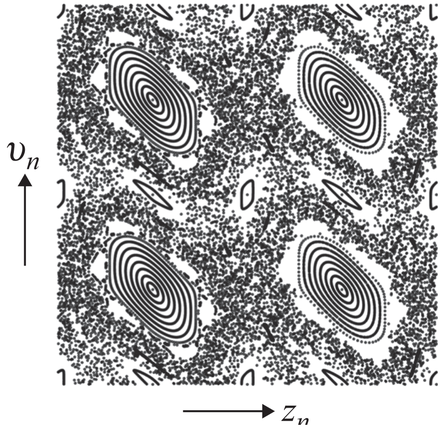

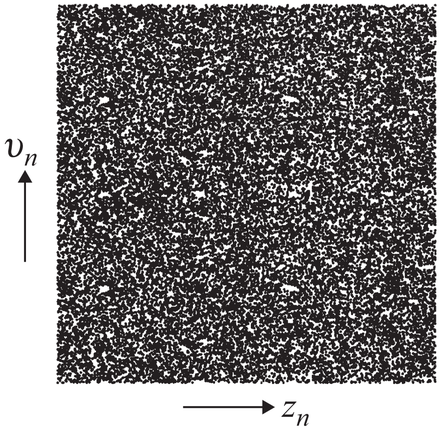

$$z_{m+1} = z_m + v_m \qquad (11.1.56)$$

$$v_{m+1} = v_m - 2\pi\epsilon^2 \sin(2\pi z_{m+1}). \qquad (11.1.57)$$

Quasilinear Velocity-Space Diffusion

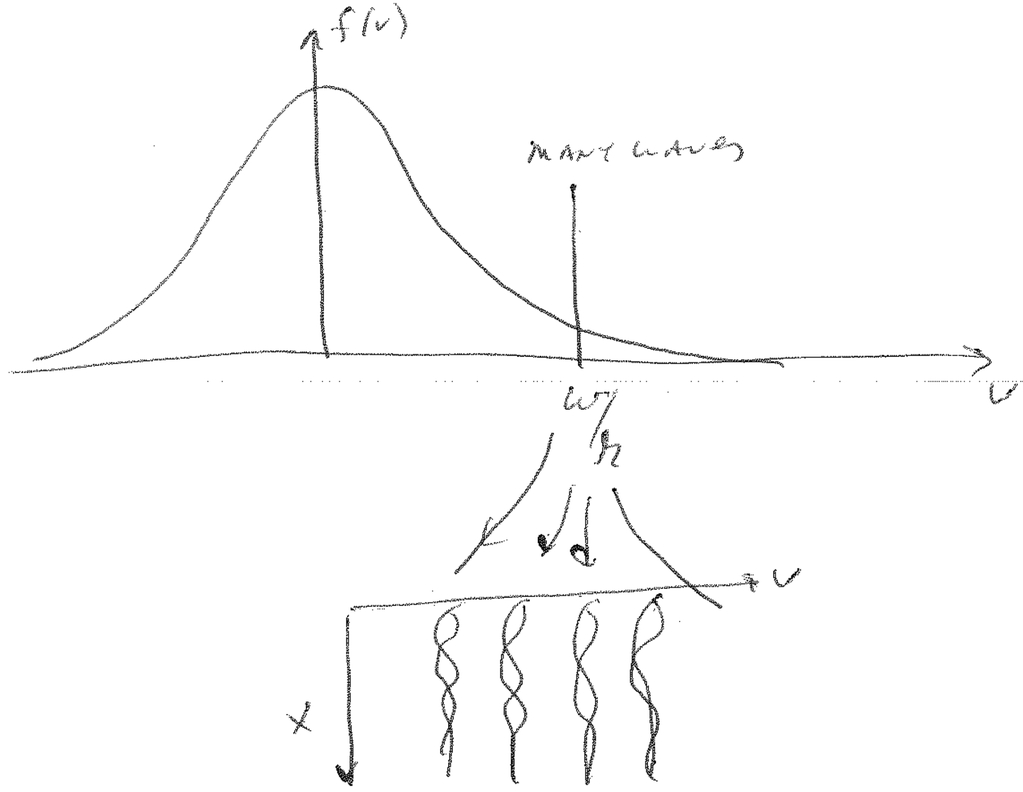

Simplify

$$\xi = kx \qquad V = \frac{kv}{\omega} \qquad \tau = \omega t$$

$$\epsilon^2 = \frac{q k E_0}{m \omega^2}$$

BOOST TO MIDDLE OF RESONANCE $(-N \ldots 0 \ldots N)$

$$\frac{d\xi}{d\tau} = V$$

$$\frac{dV}{d\tau} = \epsilon^2 \sum_{-N}^{N} \cos(x - n\epsilon)$$

$$\frac{dx}{dt} = v$$

$$\frac{dv}{dt} = \frac{q}{m} E_0 \sum_{N} \cos(k_n x - \omega_n t + \phi_n)$$

← N RANDOMLY PHASED WAVES

Quasilinear Velocity-Space Diffusion

$$\sum_{-N}^{N} \cos(x - nt) = \cos(x)\,\frac{\sin\left((N+\tfrac{1}{2})\epsilon\right)}{\sin\left(\epsilon/2\right)}$$

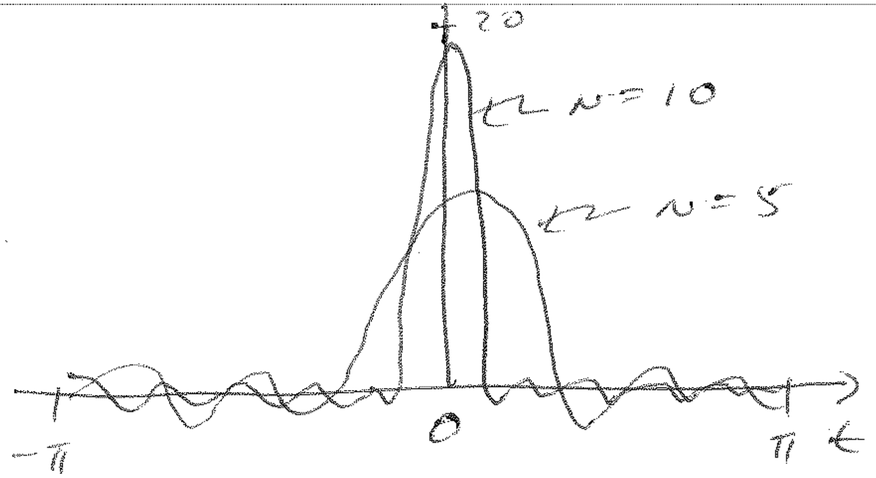

NET FORCE IS APPLIED AT $\epsilon = 0$ ACCELERATION LIKE A DELTA FUNCTION

STANDARD MAP

$$\frac{dx}{dt} = v \quad \Longrightarrow \quad x_{n+1} - x_n = v_n$$

$$\frac{dv}{dt} \cong 2\pi\epsilon^2 \cos(x) \sum_{-N}^{N} \delta(t - 2\pi n)$$

OR

$$v_{n+1} - v_n = -2\pi\epsilon^2 \sin(2\pi x_{n+1})$$

$$x_{n+1} = x_n + v_n$$

$$v_{n+1} = v_n - 2\pi\epsilon^2 \sin(2\pi x_{n+1})$$

$v = 0$ WHEN $2\pi x_{n+1} = 2\pi, 4\pi, \ldots$ FIXED POINTS

PERIODIC

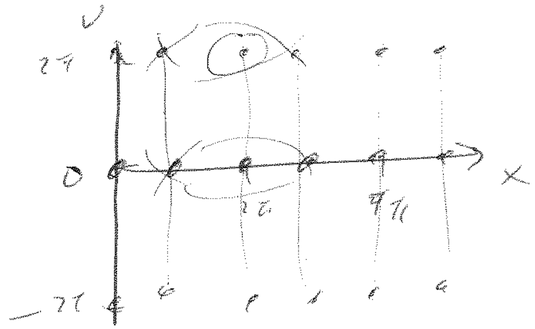

Quasilinear Velocity-Space Diffusion

```
sMap[κ_][{x_, v_}] :=
 {Mod[x + v, 2 π, -π], Mod[v - κ Sin[x + v], 2 π, -π]}
```

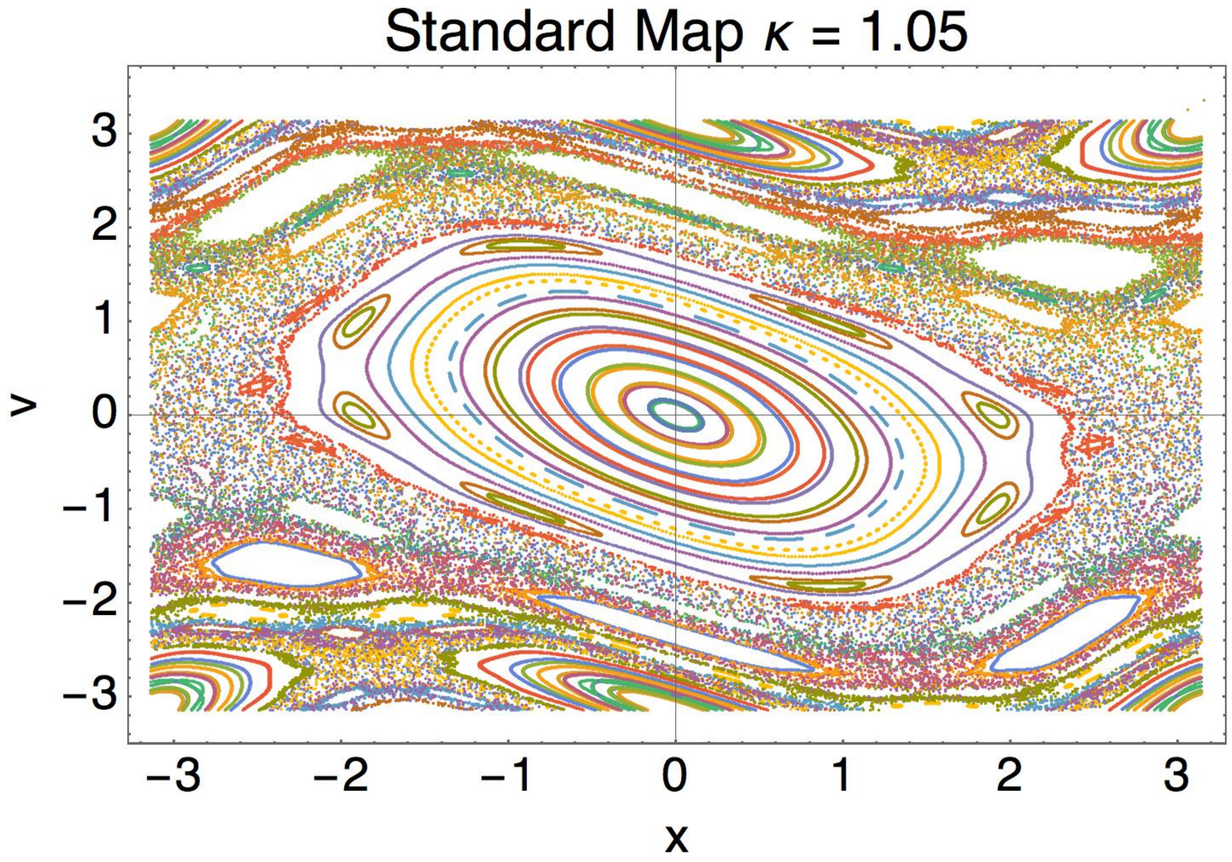

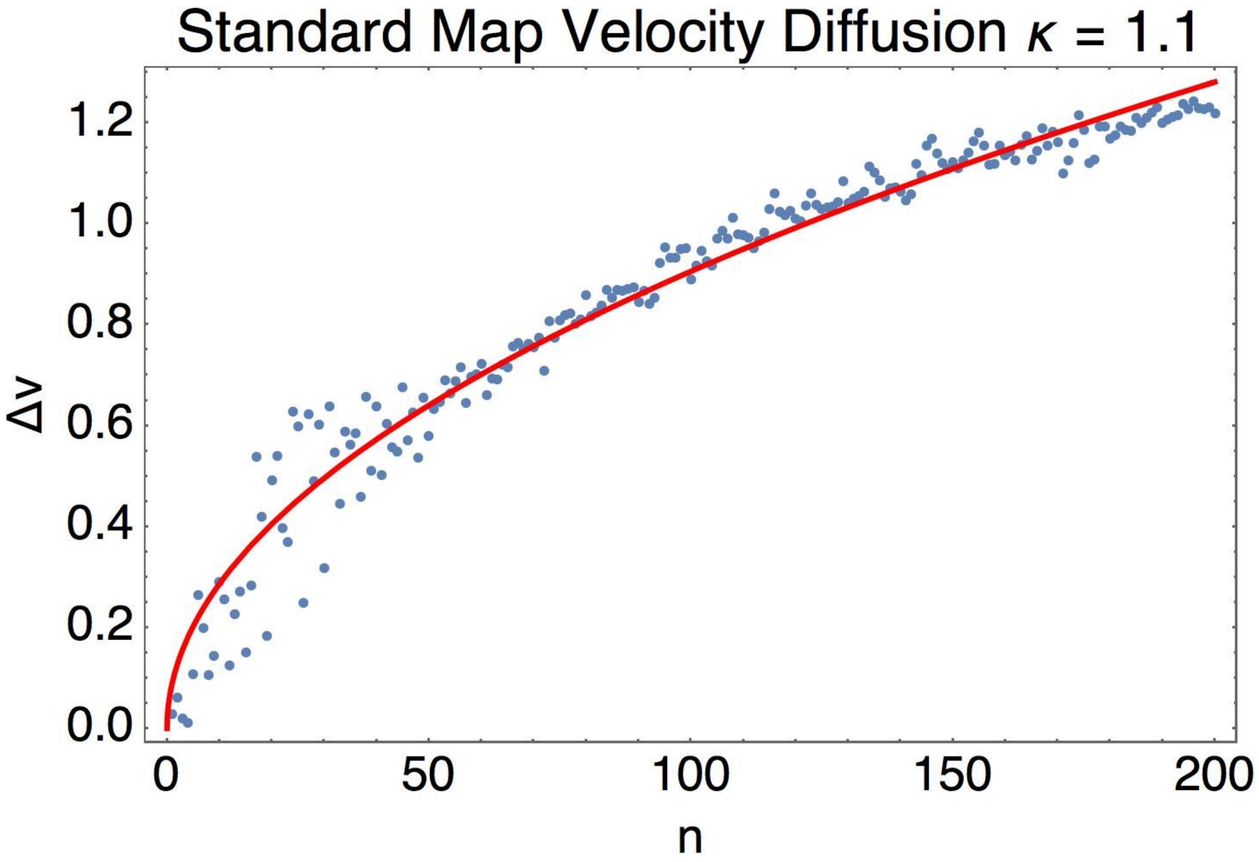

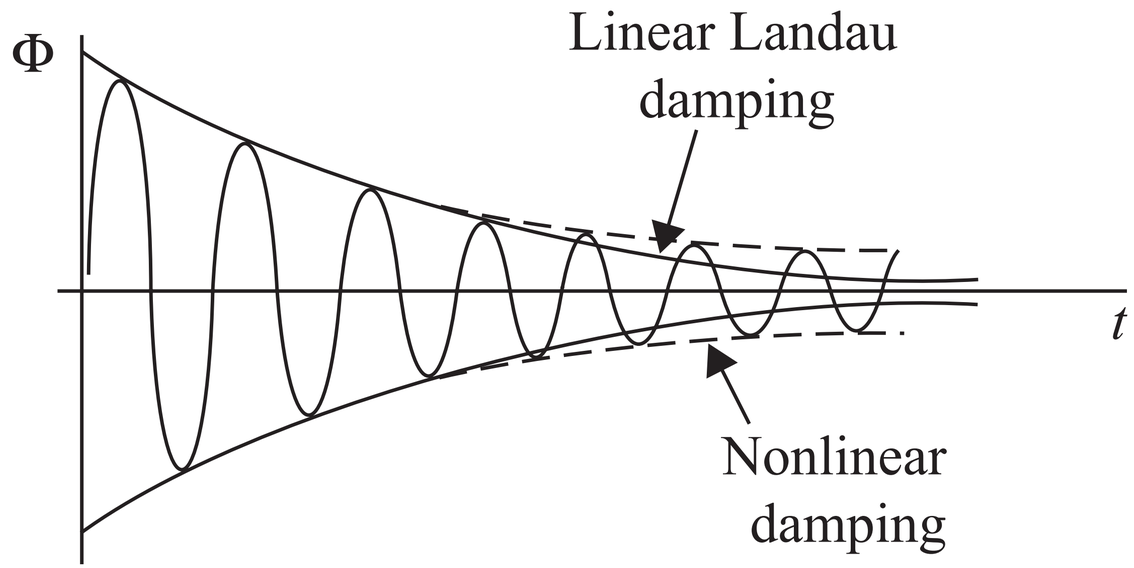

Figure 9.15 The nonlinear effects of particle trapping tend to increase the wave amplitude relative to the predictions of linear Landau damping.

Physics of Fluids 13 , 2422 (1970); [https://doi.org/10.1063/1.1693255]

Nonlinear Development of the Beam–Plasma Instability

W. E. DRUMMOND
University of Texas at Austin, Austin, Texas 78712
J. H. MALMBERG
Gulf General Atomic Incorporated, San Diego, California and
University of California, San Diego, La Jolla, California 92037
T. M. O'NEIL
University of California, San Diego, La Jolla, California 92037
AND
J. R. THOMPSON
University of Texas at Austin, Austin, Texas 78712
(Received 12 January 1970; final manuscript received 27 April 1970)

The nonlinear limit of wave growth induced by a low density cold electron beam in a collisionless plasma is calculated from a simple physical model. The bandwidth of the growing "noise" is so small that the beam interacts with a nearly sinusoidal electric field.

Experimental Test of Quasilinear Theory*

C. Roberson, K. W. Gentle, and P. Nielsen
Center for Plasma Physics, University of Texas, Austin, Texas 78712
(Received 5 November 1970)

The shape and amplitude of the electron-plasma wave spectrum resulting from a "gentle bump" on the tail of the electron velocity distribution of a plasma is measured and found to be in good agreement with quasilinear theory.

In this Letter we report an experiment designed to test the validity of this theory by measuring the electron-plasma wave spectrum resulting from the injection of an electron beam of sufficiently low density and large velocity spread to satisfy the assumptions of quasilinear theory. In prior beam-plasma experiments the initial velocity spread of the beam electrons was not sufficient to meet the requirements.[3-5]

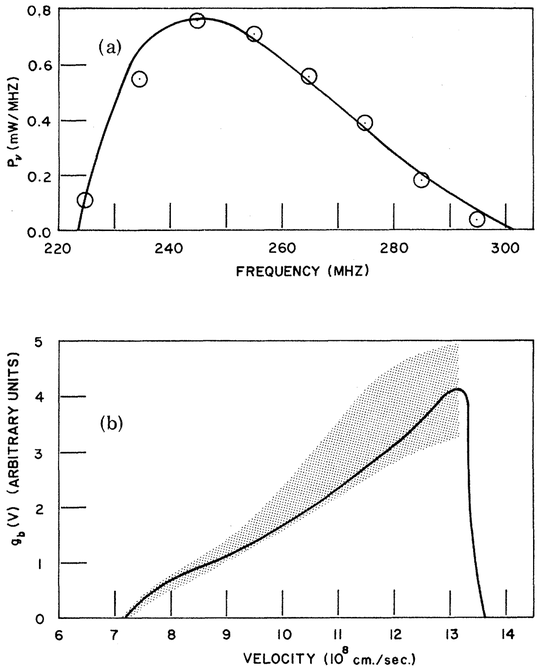

FIG. 3. (a) Shape of wave spectrum. Solid line is theory, circles are experimental values. Beam current is 2 mA. (b) Inferred beam-velocity distribution versus energy analyzer distribution. The solid curve is obtained from an electronically differentiated output of the analyzer.

Experimental Test of Quasilinear Theory*

The plasma is produced by ionization of hydrogen gas in a coaxial stub microwave cavity, and it drifts along magnetic field lines down a 250-cm aluminum tube 10 cm in diameter. The plasma is terminated by a plate with a $\frac{3}{4}$-cm hole behind which the electron gun is mounted. The plate is biased to reflect electrons with velocities less than the slowest of those that come from the gun. The tube acts as a waveguide beyond cutoff for electromagnetic propagation at the wave frequencies used, and has four longitudinal slots equispaced around the circumference along which antenna probes may be moved. The complete assembly is contained in a vacuum chamber and maintained at a pressure of less than 10^{-5} Torr by diffusion and Ti sublimation pumps. Axial magnetic field coils are mounted around the vacuum chamber and provide a magnetic field of about 1 kG. The electron gun is a simple diode with a large-aperture (2.5-cm diam) plate mounted inside a soft-iron cylinder. The result is a beam distribution with a large spread in parallel energy, which when injected into the plasma makes a bump on the tail of the parallel electron-velocity distribution. The energy distribution of the beam is measured directly using a large-aperture gridded energy analyzer.

The dispersion curve is determined from measurements of wavelength as a function of the frequency of the plasma wave. The wavelength can be observed directly by adding a constant-phase reference signal from the transmitter to the received signal. As the receiving probe is moved, the interference pattern is plotted on an X-Y recorder, displaying the wavelength. The temperature and density of the plasma are inferred by computer using a program that solves Eq. (1) to obtain the best least-squares fit to the experimental points. The beam may be turned on and the dispersion data repeated using coherent detection to find the test wave in the noise spectrum. The wavelengths may be compared with those measured without the beam to show that the beam does not change the dispersion relation. The results are shown in Fig. 1.

Experimental Test of Quasilinear Theory*

The dispersion curve is determined from measurements of wavelength as a function of the frequency of the plasma wave. The wavelength can be observed directly by adding a constant-phase reference signal from the transmitter to the received signal. As the receiving probe is moved, the interference pattern is plotted on an X-Y recorder, displaying the wavelength. The temperature and density of the plasma are inferred by computer using a program that solves Eq. (1) to obtain the best least-squares fit to the experimental points. The beam may be turned on and the dispersion data repeated using coherent detection to find the test wave in the noise spectrum. The wavelengths may be compared with those measured without the beam to show that the beam does not change the dispersion relation. The results are shown in Fig. 1.

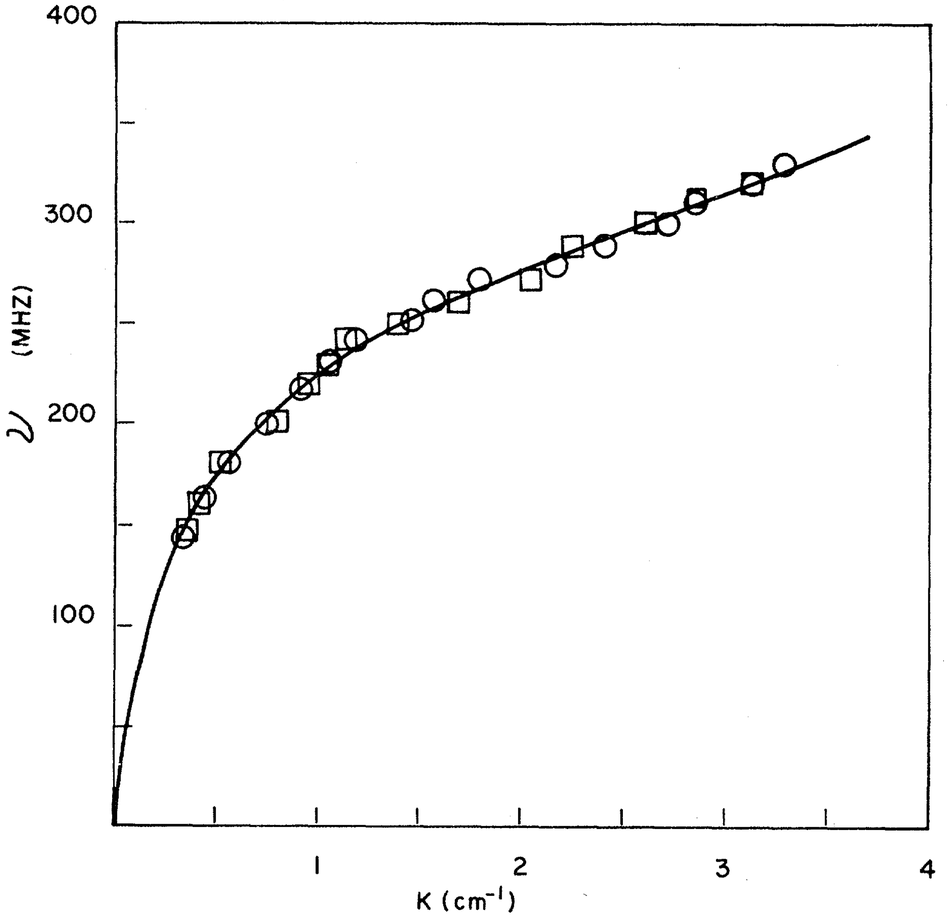

FIG. 1. Dispersion curve. The solid line is calculated without beam, circles are observations without beam, squares are observations with a beam current of 2.6 mA. The electron temperature is 14 eV. The central electron density is 1.3×10^{9} electron/cm^{3} with a half-width of approximately 3 cm.

Experimental Test of Quasilinear Theory*

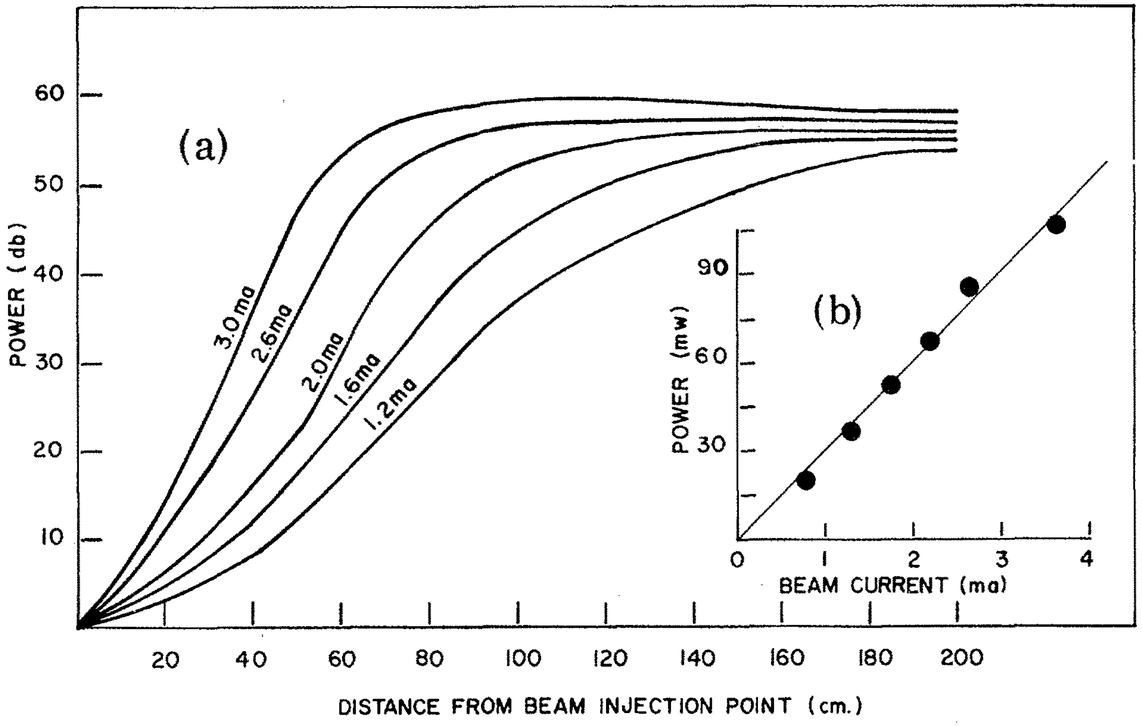

FIG. 2. (a) Wave growth and saturation versus distance. (b) Saturation power level versus beam current.

The spatial growth of the noise as a result of the beam is measured by connecting the receiving antenna directly to a broad-band amplifier and a sampling rf voltmeter. The log of the voltmeter output is plotted on the Y axis and distance from beam injection point on the X axis of the recorder. The results [Fig. 2(a)] have the qualitative features expected from the theory: slow exponential growth to reach a quasiequilibrium saturation level without overshoot.

Experimental Test of Quasilinear Theory*

small to justify this easily. This inferred beam distribution is compared with the direct measurement using an energy analyzer. The results are shown in Fig. 3(b), where the width of the shaded region is an indication of the estimated error in determining the inferred distribution. No "normalization" procedure is used in this comparison.

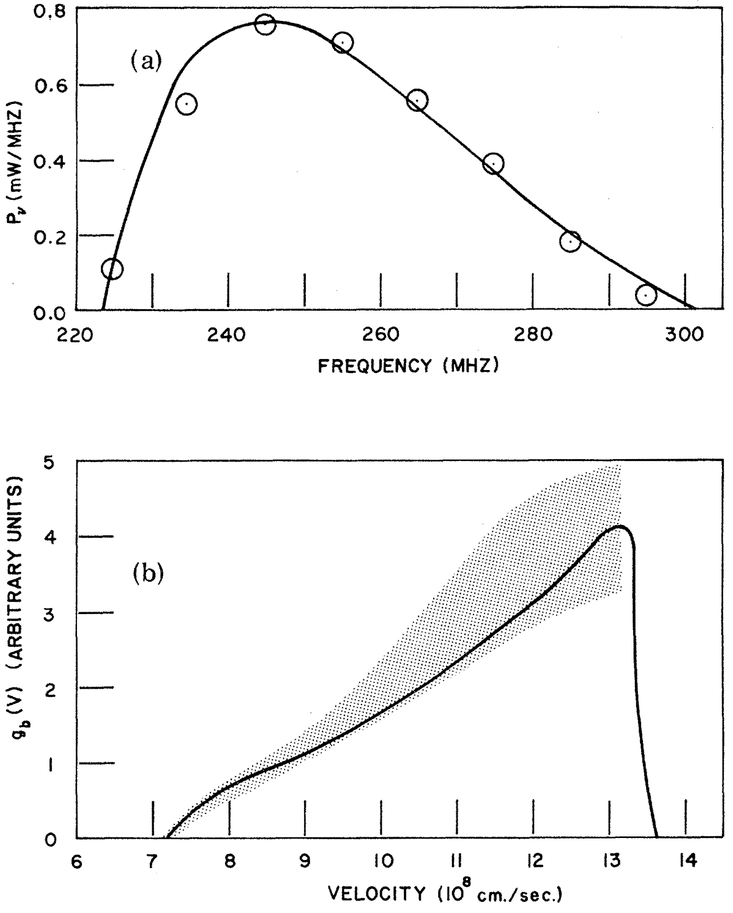

FIG. 3. (a) Shape of wave spectrum. Solid line is theory, circles are experimental values. Beam current is 2 mA. (b) Inferred beam-velocity distribution versus energy analyzer distribution. The solid curve is obtained from an electronically differentiated output of the analyzer.

Next Week

10

Waves in a Hot Magnetized Plasma

$$\mathbf{v}\times\mathbf{B}_0\cdot\boldsymbol{\nabla}_{\mathbf{v}}f_{s0}=0 \tag{10.1.2}$$

$$\frac{\partial f_s}{\partial t}+\mathbf{v}\cdot\boldsymbol{\nabla}f_s+\frac{e_s}{m_s}(\mathbf{v}\times\mathbf{B}_0)\cdot\boldsymbol{\nabla}_{\mathbf{v}}f_s+\frac{e_s}{m_s}[\mathbf{E}+\mathbf{v}\times\mathbf{B}]\cdot\boldsymbol{\nabla}_{\mathbf{v}}f_{s0}=0, \tag{10.1.3}$$